CHAPTER 5

Detection of limonin using CeO_2 NPs based IDE capacitive sensor

Contents

5.1. Introduction

The rapid and onsite detection of limonin concentration is essential to make the fruit juice product acceptable to the commercial market. The CeO_2 NPs were synthesized through a low-cost and eco-friendly method using Dillenia Indica (D. Indica) aqueous extract as explained in the preceding chapter 4 and the capacitive sensor was fabricated by drop coating of CeO_2 NPs on IDE structure patterned on paper substrate. Here, the focus has been given to the rapid, accurate and onsite measurement of limonin concentration in citrus limetta and citrus grandis fruit juices using CeO_2 NPs based capacitive sensor. The nanostructure (CeO_2) here increases the surface area of the sensor enhancing its sensing performance. The planar interdigitated structure has been used for exhibiting fast response, small in size, inexpensive and providing no radiation that is harmful [1, 2]. Recently, Au/Ti electrodes IDE structure based gas and humidity sensors have been reported to exhibit a fast response and recovery behavior with a large temperature range [3-6]. Hence, observing the advantages of IDE, we have aimed to develop a capacitive sensor based on IDE structure on a flexible substrate utilizing CeO_2 NPs as a sensing material for the quantification of limonin in citrus fruit juices (Citrus limetta and Citrus grandis or Citrus maxima).

5.2 Materials and Methodology

5.2.1 Materials

Standard Limonin powder was procured from Sigma Aldrich. The other chemicals such as citric acid, ascorbic acid, and sugars of analytical grade were procured from Alfa Aesar company. The polyvinyl alcohol (PVA) powder was purchased from Alfa Aesar company. Acetonitrile and tetrahydrofuran of HPLC grade were purchased from the same Alfa Aesar company. In our work, citrus limetta and citrus grandis fruit juices were used as the target analytes in finding out limonin concentration. The fruits were procured from Tezpur, Assam, India

5.2.2 CeO_2/PVA composite

For the preparation of polymer nano-composite, appropriate wt% of PVA powder (500 mg) was mixed with 10 ml of Deionized (DI) water and stirred vigorously at 400 rpm for 3 h at 80 ℃ until a clear solution was achieved. CeO_2 powder was sonicated in water (1.0 g CeO_2 powder and 4.0 ml of DI) for 10 mins. Then the solution of CeO_2 was dropped slowly into 10 ml of aqueous PVA solution and stirred (400 rpm) at room

temperature for 20 mins until the homogeneous dispersion was obtained. Thus, a viscous gel of CeO_2/ PVA composite obtained was used for the deposition over the sensor substrate.

5.2.3 Preparation of Citrus fruit juice extracts

The Citrus fruits-Citrus limetta and Cirus grandis were taken for analysis purposes due to their availability and possible storage as a juice product. The fruits were cut into pieces after being washed under running water. After that, it was crushed and juiced and for five minutes, the juice was centrifuged at 1000 rpm. After filtering the clear solution with Whatman 1 filter paper, the filtrate was used to carry out further investigation.

5.2.4 HPLC analysis

Citrus limetta and Citrus grandis fruit juices were analyzed analytically utilizing the C18 column by HPLC (shown in Fig. 5.1) to determine their limonin concentration. The following components: a C18 column guard, two hydraulic pumps (515), an injection system, UV visible detection (2489), and a computerized recorder/integrator comprise the HPLC system (Water Corporation, USA). Before juice was injected into the HPLC system, the juice extract was diluted with HPLC-grade methanol in 1:2 ratio and then filtered using a 0.45 µm nylon (Polytetrafluoroethylene) PTFE filter. An isocratic system was used to detect limonin, with a flow rate of 0.5 ml/min and a run time of 10 mins. The mobile phase solvent was a combination of acetonitrile, tetrahydrofuran, and deionized water in the ratio 17.5-17.5-65 (v/v/v). The detecting wavelength was set at 207 nm and the injection volume was 20 µl [7]. All working standards were prepared from standard limonin as 20 ppm, 15 ppm, 10 ppm, 5 ppm and 1 ppm using HPLC grade methanol. HPLC analysis was performed and the concentration of limonin was estimated from HPLC using the relation (5.1) [8].

$$Con._{unknown} = (A_{unknown}/ A_{standard})\ Con._{standard} \qquad (5.1)$$

where $Con._{unknown}$ is the concentration of unknown, $A_{unknown}$ is the area under the curve of unknown, $A_{standard}$ is the area under the curve of standard sample and $Con._{standard}$ is the known standard's concentration.

5.2.5 Sensing mechanism

The CeO_2 NPs based IDE sensor's response depends on the interaction of ionic groups present in limonin and the oxygen vacancies present in the CeO_2 NP fcc crystal

Figure 5.1: HPLC setup

structure (Fig. 5.2). Cerium is an abundant rare earth metal that exists in two oxidation states (+3 and +4) belongs to lanthanide series [9]. The oxide of Cerium (CeO_2) represents the cubic fluorite structure with oxygen deficiencies showing redox reaction sites [10]. Though cerium oxide has a mix of 3+ and 4+ states at the nanoscale, the number of 3+ sites decreases with a decrease in particle size [11]. The oxygen vacancies react with the ions of electro active components [12]. The antioxidant compound such as limonin possesses electro active ions [13, 14] interacting with the oxygen vacancies of Ce resulting in the change in the capacitance (Fig. 5.2). The hydrogen (electron) donating

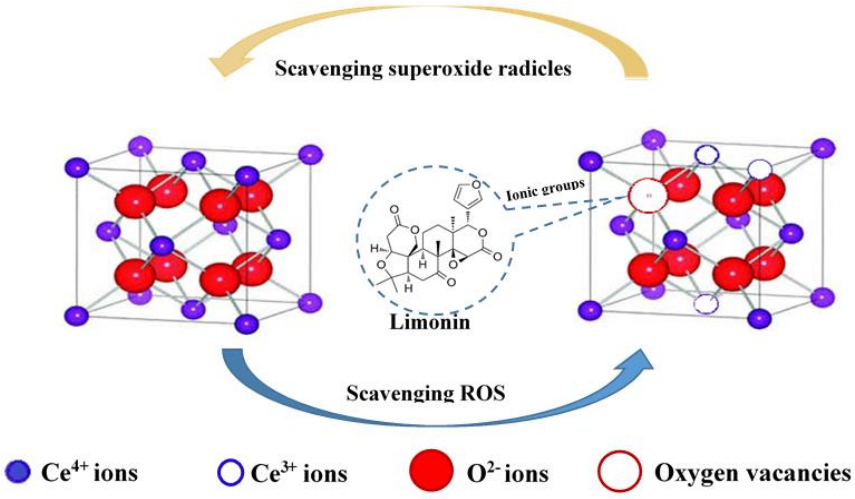

Figure 5.2: Sensing Mechanism of Limonin and CeO_2 NPs

ability of a limonoid and flavonoid molecule act to scavenge a reactive radical species [14]. Considering this advantage of CeO_2, we have used CeO_2 NPs in the interdigitated capacitive sensor for sensing limonin concentration that contributes to delayed bitterness. The anti-oxidative properties of limonin facilitate the generation of capacitance in the

electrode structure of IDE. The composition of Ce in two oxidation states and its interaction with the analyte limonin is shown in Fig. 5.2. The interaction of limonin with the vacancies of CeO_2 NPs were used for the limonin quantification utilizing an IDE-based capacitive sensor.

5.3 Results and Discussion

5.3.1 Calibration

The sensor was calibrated for different limonin concentrations at room temperature, ranging from 1 ppm to 20 ppm (Fig. 5.3a and 5.3b). The transfer characteristic of the capacitive sensor was obtained with capacitance C^S_{sam} versus concentrations of limonin (1-20 ppm) showing a linear increase in capacitance with the increasing concentration of limonin (Fig. 5.3b). The standard deviation (SD) which is a measure of how dispersed the data is in relation to the mean was calculated. The SD is calculated using the formula $SD = \sqrt{\frac{\sum|X_1-\mu|^2}{N}}$, where SD is the standard deviation, X_1 is the data point we are solving for in the set, μ is the mean, and N is the total number of data points. The standard deviation (SD) for each curve in Fig. 5.3a considering the point from gaining saturated values are ±5.4μF (for 1ppm), ±7μF (for 5 ppm), ±18μF (for 10ppm) and ±21μF (for 20 ppm). The regression analysis for the transfer characteristics in Fig. 5.3b exhibits a regression coefficient, R^2 =0.982. The regression curve is represented by the dotted line in Fig. 5.3b and is characterized by Eq (5.2)

$$y= 9692998.93*x+1.81042E7 \quad (5.2)$$

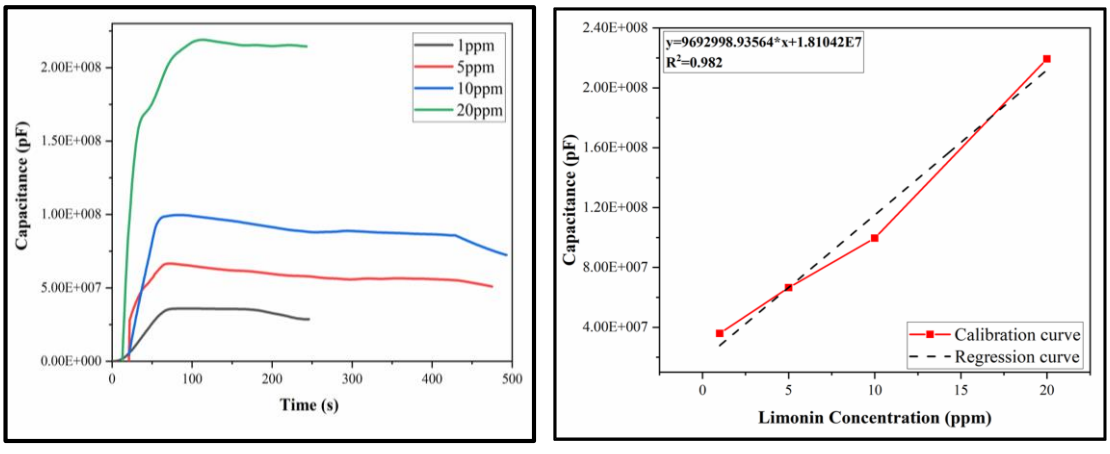

(a) (b)

Figure 5.3: (a) time dependant analysis for the sensor at different concentrations of limonin standards (b) calibration curve with regression analysis

Here, y represents the C^S_{sam} and x is the limonin concentration. The regression value R^2 =0.982 indicates a very small deviation from the experimental result of the IDE device using CeO_2. The curve is very close to a straight line showing a linear increase of capacitance with the concentration of limonin.

The residual standard deviation also referred to as the residual standard error, is a statistical indicator of how much the data deviate from the regression line that was fitted. It is determined by applying Eq. 5.3:

$$s(r)=\sqrt{\frac{\sum_{i=1}^{n}(y_i-y_i^*)^2}{n-2}} \tag{5.3}$$

where y_i^* is the value of y predicted by the equation of the calibration line for a given value of x, n is the number of calibration points, and y_i is the observed value of y for a given value of x.

Table 5.1: Calculation for the prediction interval

Concentration in ppm, x	Capacitance(μF), y_i	Predicted, y_i^*	Residual, $(y-y_i^*)$	Residual, $(y_i-y_i^*)^2$	S(r)
1	35.95	27.79	8.16	66.59	7.87
5	66.49	66.56	-0.07	0.0049	
10	99.64	115.03	-5.39	29.05	
20	219.27	213.96	5.31	28.19	

Instead of computing the whole standard error of prediction, the residual standard deviation is utilized to measure the level of uncertainty in estimated concentration values. The residual standard error obtained for our calibration is 7.87 (Table 5.1) which predicts the uncertainty in estimated values.

Table 5.2: Residual plot

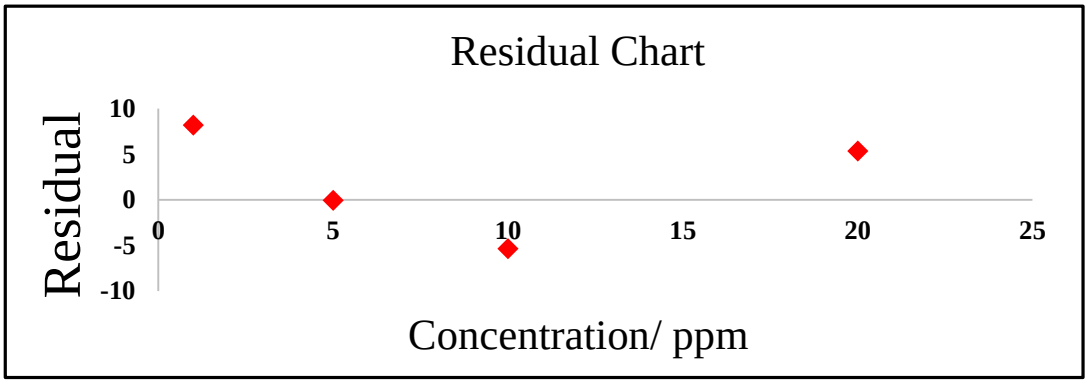

Table 5.2 shows the residual plot for the residual values ($y- y_i^*$) obtained (Table 5.1) for different concentration limonin standards. The chart is showing deviation of observed values from the predicted value with the highest deviation for 2 ppm standard limonin.

The sensor's capacitance measurements both with and without the application of the target analytes are C_{sam} and C_{in} respectively through transient analysis. The relative capacitance in terms of response is written as

$$\text{Response} = (C^S_{sam} - C_{in})/ C_{in} \quad (5.4)$$

where, C^S_{sam} is the saturated value of C_{sam} obtained from the transient capacitance response curve (Fig. 5.3a). The capacitance C_{sam} increases with time and gets almost saturated at the time of ~15 s and the saturated value of capacitance increase with an increase of limonin concentration due to having more interaction of oxygen vacancies of Ce at higher concentration of limonin (Fig. 5.2).

5.3.2 Performance analysis

As discussed in chapter 1 and 2, pomelo (Citrus grandis) and mosambi (Citrus limetta) are highly nutrient fruits due to the content of phytochemicals showing antioxidant antiviral, and antibacterial properties. The problem associated with the storage of these fruit juices for long period creates difficulty in the fruit industry. Here sample analytes from the above fruits were chosen for the performance analysis of the sensor while monitoring the limonin content causing delayed bitterness in the juice products. The sensor's performance was analyzed by studying its sensitivity, accuracy, specificity, reusability, response time, etc. Due to the interaction of CeO_2 NPs with limonin affecting the capacitance of the fabricated sensor, an attempt has been made to measure the concentration of limonin in fruit juices.

5.3.2.1 Sensitivity

The slope of the output characteristic curve (Dy/Dx in Fig. 5.3b), or, more generally, the smallest input of a physical parameter that would result in a measurable output change, is used to define a sensor's sensitivity. Some sensors describe sensitivity as the change in an input parameter necessary to generate a consistent change in output. Others define it as an output signal change in response to a specific change in an input parameter. The sensitivity of our sensor is estimated as ~ 9.62 ±0.095 µF/ ppm by using Eq. (5.2) from Fig. 5.3b. Increased sensitivity enables the identification of a small fraction of the target and lowers the limit of detection (LOD). Regardless of the target's nature,

incorporating materials with a large surface area is frequently employed to enhance sensitivity [15].

5.3.2.2 Selectivity and detection limit

Selectivity, which is measured as the ratio of the sensor signal caused by the target analyte to the interference particles (target/interference), is the ability to detect the target molecule among the mixture. Selectivity improvement improves target recognition while reducing false-positive responses. The two broad categories of methods for increasing selectivity are physical modification and chemical modification. Physical alterations include altering the physical characteristics, such as surface morphology and structure, or by adding physical barriers, such as membrane-coated microchannels, which only allow the target to pass through and reach the sensor layer [16]. The addition of materials that give target recognition, which is selected based on the target gas molecule, is a chemical modification used to improve selectivity. Chemical modification approaches offer more selectivity and consequently higher applicability compared to physical methods, despite the complex operating mechanism and selection criteria [17]. Catalyst decoration, composite formation, and surface functionalization are different methods or modifications used to increase the selectivity of sensor devices [18]. Here the sensor is fabricated with the adsorption material (CeO_2 NPs) for selective adsorption of limonin in target juice samples. The selectivity is further lifted by following the composition method

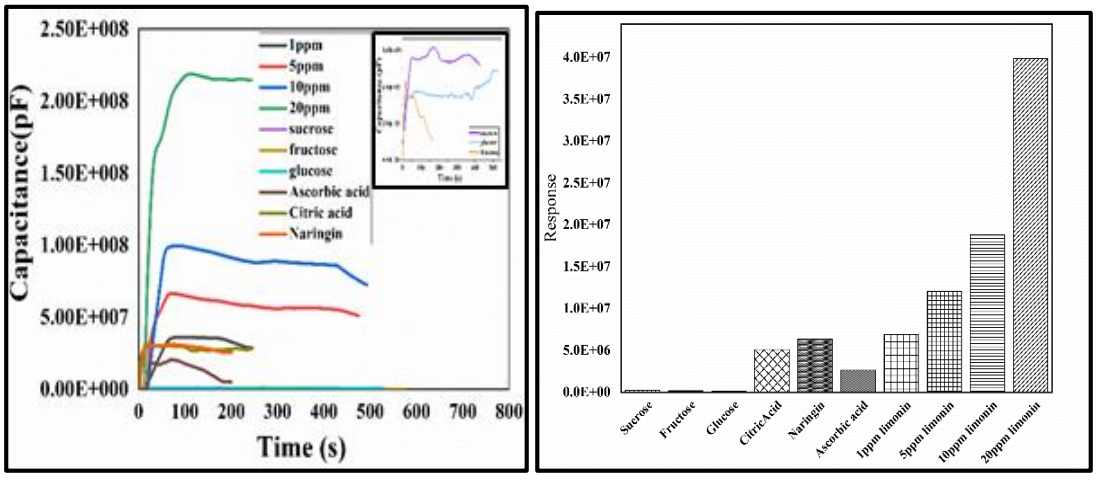

(a) (b)

Figure 5.4: (a) Time dependant selectivity study with interfering compounds tested independently (b) columns showing gradual increase in capacitance response for limonin with insignificance change with respect to other interfering compounds.

utilizing polymer along with the NPs in the sensor. For the selectivity study of the sensor, we prepared the aqueous solutions of major non-volatile components containing 0.158 M fructose, 0.173 M sucrose, 0.329 M glucose, 2.78 mM ascorbic acid, 26.03 mM citric acid, and 367.3 µM naringin [19]. The mole concentration of limonin in an aqueous solution varied from 2.1253 µM to 42.51 µM (1 ppm to 20 ppm). After exposing the sensor to these solutions, the transient capacitance curves (Fig. 5.4a) of a Ceria Nanoparticles (CNP)-PVA-based sensing device exhibit higher saturated values (C^S_{sample}) for limonin solutions than that of other solutions due to the strong interaction of limonin with CeO_2 in comparison to other solutions indicating high selectivity of limonin sensing by the IDE sensor. From Fig. 5.4a and Fig. 5.4b, the response values of capacitance obtained by Eq. (5.4) reveal a weak dependence of the sensor's output on the other components present in the juice compared to limonin solutions.

The ability of a method/device to detect the presence or absence of analytes in samples at which detection is feasible is known as the limit of detection (LOD)[20]. This can be calculated using the standard deviation (σ) of the repeated analysis using blank samples and the slope of the calibration equation (b) as follows:

$$\text{limit of detection} = 3\,\sigma/b \qquad (5.5)$$

The value of LOD as calculated using Eq. 5.2 and Eq. 5.5 is 5.462 µM. As shown in Fig. 5.5 the solution below 90 ppb of limonin exhibits response values that are nearly identical to those of DI water. Above 90 ppb of limonin (standard solution), the sensor shows a substantial change in comparison to that for only DI water. The minimum value (approx.) for limonin detection in citrus juices is assessed as ~100 ppb for the sensor considering experimental study only.

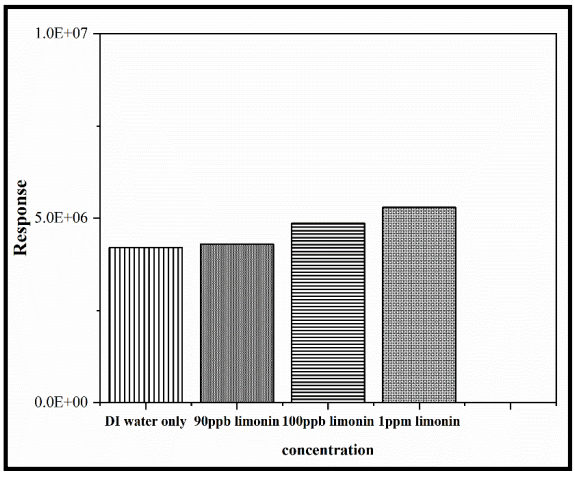

Figure 5.5: Response of sensor shows Bars representing sensor's response to DI water and limonin conc (90 ppb, 100 ppb. 1ppm)

5.3.2.3 Limonin detection and accuracy study

The developed sensor was tested to detect limonin concentration in juice samples of citrus limetta and citrus grandis at different storage times after its preparation such as at the time of its preparation (0 h) and after a storage time of 6 h and 10 h. The concentration of limonin in juice increases with storage time indicating enhancement of

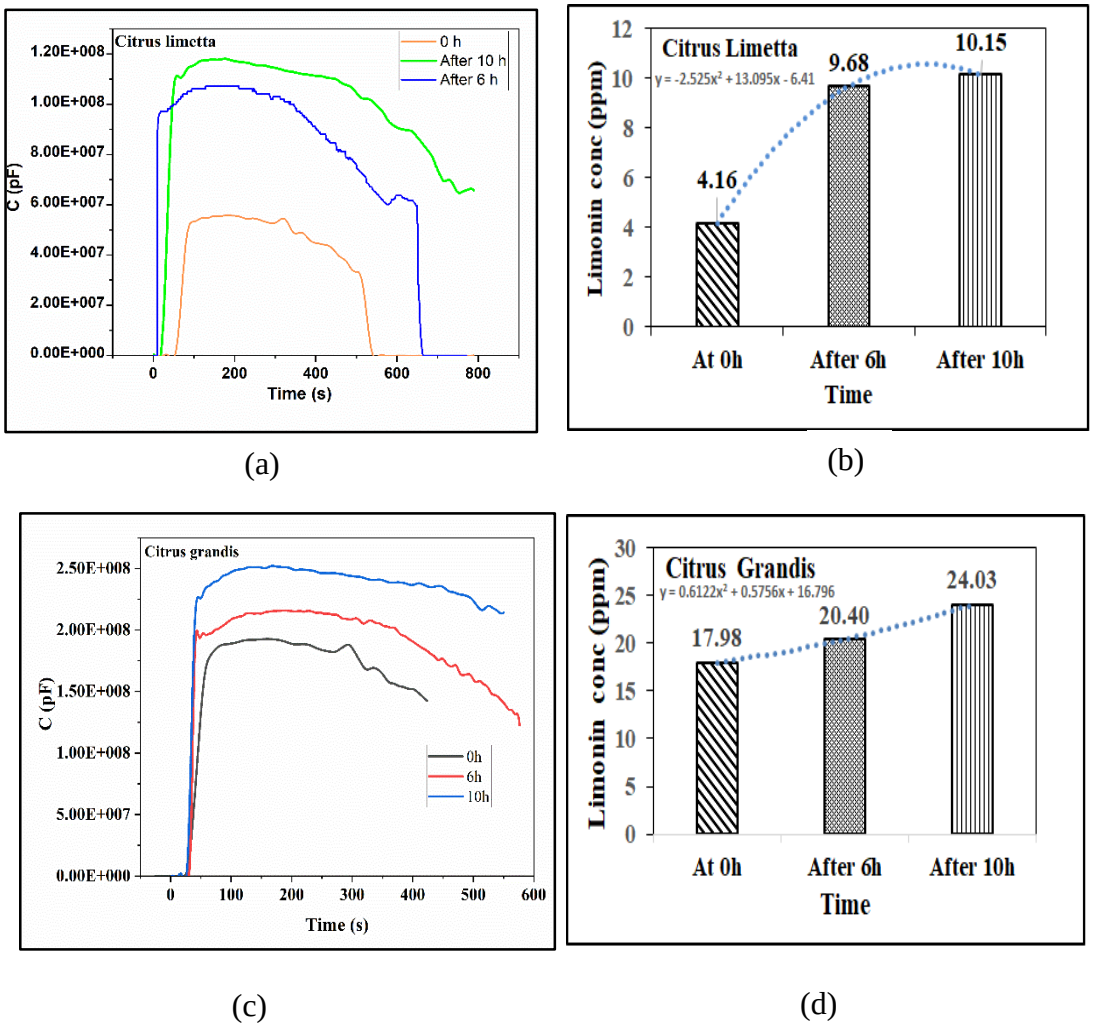

Figure 5.6: (a) time domain analysis of Citrus llimetta juice sample at different time interval after juice preparation at RT (b) limonin content in Citrus llimetta juice sample calculated at different time period (c) time domain analysis of Citrus grandis juice sample at different time interval after juice preparation at RT (d) limonin content in Citrus grandis juice sample calculated at different time period

the bitterness with time. The transient response in Fig. 5.6a shows the increase in capacitance with time and the capacitance gets saturated at ~ 13 s. With an increase in storage time, C^{S}_{sam} also increases. The SD obtained for each of the curve of Fig 5.6a are ±6.91µF, ±15.80µF and ±18.99µF for 0h, 6h and 10h respectively ignoring the capacitance for inicial rise. The amount of limonin in the Citrus limetta juice was estimated as ~ 4.16 ppm, 9.68 ppm and 10.15 ppm for as- prepared juice at 0 h, at 6 h and

10 h of storage samples respectively using our sensor (Fig. 5.6b). The polynomial $y=-2.252x^2+13.095x-6.41$ as in Fig. 5.6b shows the trend line for increase in limonin content with time. The limonin content at different times such as at 1h, 2 h, 3 h are predicted as 5.5 ppm, 6.17 ppm.7.75 ppm respectively as obtained from the increasing trend in Fig. 5.6b.

Table 5.3: Real-time domain analysis using sensor and HPLC analysis for accuracy measurement for *citrus limetta*:

Cycle no	Sensor based analysis for *citrus limetta*		HPLC analysis for *citrus citrus limetta*		Accuracy(percentage error)
	Limonin conc.(ppm)	Percentage increase from initial value (approximate)	Limonin conc.(ppm)	Percentage increase (approximate))	
At 0 h	4.16	0%	$\frac{0.02128}{0.04353} x10$ =4.89	0%	14.92%
After 6 h	9.68	132 %	$\frac{0.0369}{0.04353} x10$ =8.48	53.9 %	14.15%
After 10 h	10.15	143%	---	----	

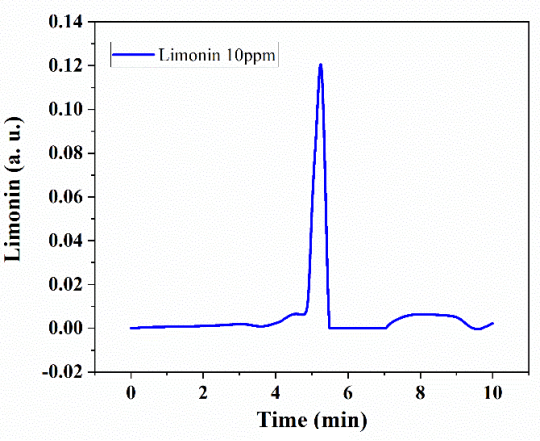

(a)

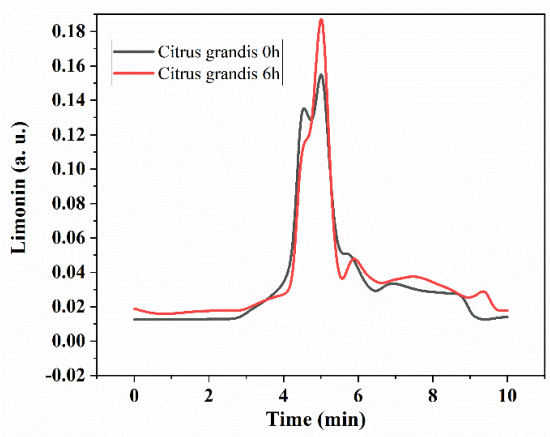

(b)

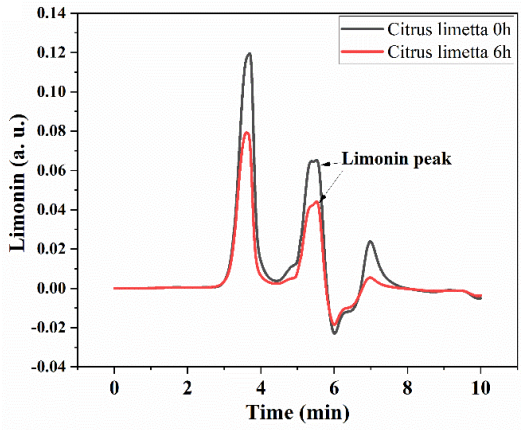

(c)

Figure 5.7: HPLC analysis for (a) standard limonin (10 ppm) (b) Citrus grandis juice sample at different time (c) Citrus llimetta juice sample at different time

The percentage of increase in limonin concentration after 6h and 10h of storage time is estimated as 132% and 143% respectively (Table 5.3). For validation of the sensor's performance, HPLC analysis of fruit juice was carried out for as-prepared and 6h storage samples to find out limonin concentration (Fig. 5.7a and Fig 5.7c).

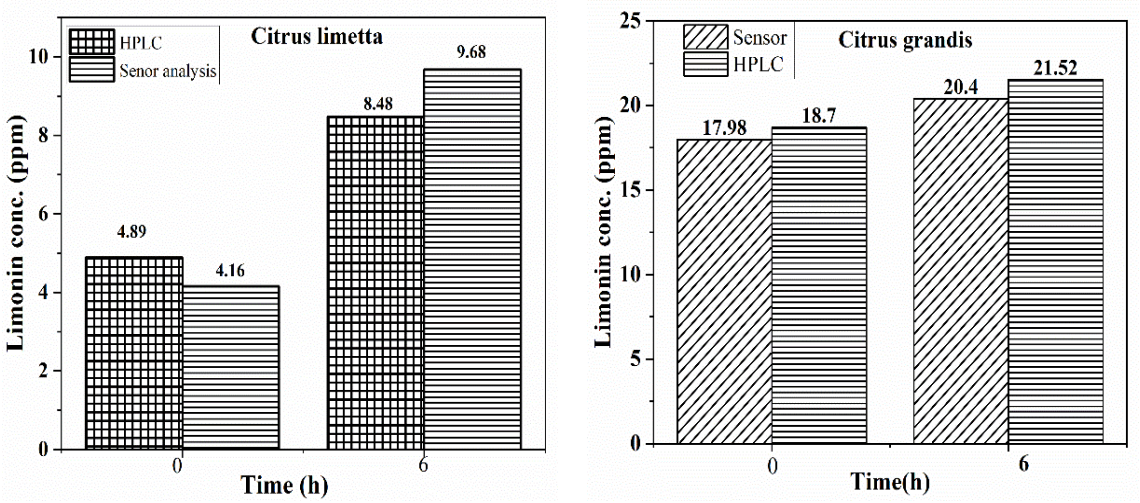

(a) (b)

Figure 5.8: Comparison of HPLC results with sensor's output

The limonin concentrations estimated from HPLC analysis are 4.89 ppm for as-prepared fruit juice (0hr) and 8.48 ppm for 6 h preserved citrus limetta sample (Table 5.3) matching closely with the results obtained by using our sensor device (Fig. 5.8a). The accuracy of the sensor is the maximum difference between the actual value (measured with primary standard, HPLC analysis) and the output measured with the developed sensor. Here, the accuracy is stated in terms of percentage deviation from the standard value obtained in HPLC analysis. The accuracy of the sensor shows a deviation (percentage error) of ≈14% with reference to the HPLC analysis (Table 5.3).

Limonin content has increased by 13.18% according to the time domain analysis used to quantify it in citrus grandis juice after 6 h of its preservation (Figs. 5.6c and 5.6d) with a SD of the curves ranges from ±16.66 (0h) to ±24.91(6h). The limonin content increased from 17.98 ppm to 20.40 ppm for 6 h of storage and finally increased to 24.03ppm with a storage time of 10h. The SD for the curve for 10h is ±25µF(approx.) The increasing trend ($y=0.61222x^2+0.57565x+16.796$) for the limonin concentration is shown in Fig. 5.6d. It reveals that an increase of approximately 0.5 ppm/h of limonin from 0 h to 6 h is observed which increases to approximately 0.9 ppm /h from 6 h to 10 h of its

storage. Moreover, as revealed in Fig. 5.8b and Table 5.4, HPLC findings were compared with sensor output where the sensor's result has a 0 - 5.20% variance to the results of HPLC analysis (Fig. 5.7b) while considering the study after 6 h of juice preservation.

Table 5.4: Real time domain analysis using sensor and HPLC analysis for accuracy measurement for *citrus grandis*

Cycle no.	Sensor based analysis For *citrus grandis*		HPLC analysis For *citrus grandis*		Accuracy(in terms of percentage error)
	Limonin conc.(ppm)	Percentage increase from initial value (approximate)	Limonin conc.(ppm)	Percentage increase (approximate)	
At 0 hr	17.98	0%	=(0.08142/0.4353)x10 =18.70	0%	3.85%
After 6 hrs of its storage	20.40	13.45 %	=(0.09369/0.4353)x10 =21.52	15.08 %	5.20%
After 10 hrs of its storage	24.03	20.18%	---	----	

5.3.2.4 Response time

When an input parameter changes, sensors do not instantaneously change their output state. Instead, it will gradually transit to the new state over time, which is referred to as the response time (T in Fig. 5.9). The duration needed for a sensor output to transition from its initial value to a final settled value that falls within a tolerance band is known as the response time. Typically it is stated as the amount of time needed to reach 90% of the final value, calculated from the moment the measured variable's step input change began [21]. Considering Fig 5.9, the response time for the sensor is calculated as response time $T_r = t_{90\% \text{ of total}} - t_{initial} = 13$ s, where $t_{90\% \text{ of total}}$= the time taken by the sensor to respond

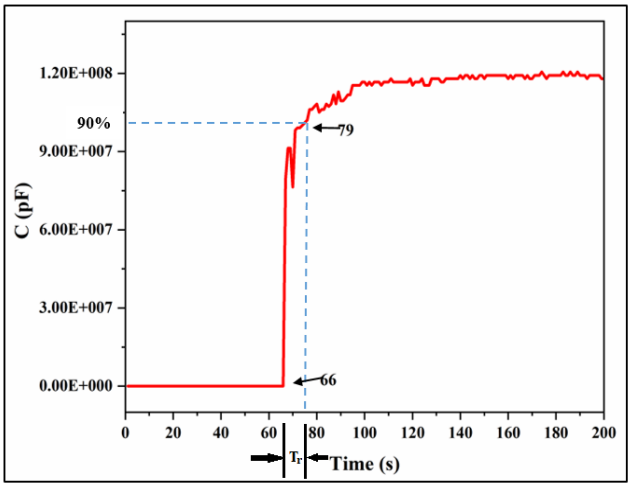

Figure 5.9: Response time calculation considering real juice sample at 0h

to the target material to reach 90% of its maximum capacitance value which is equal to 79 s and $t_{initial}$=time required to get initial response = 66s.

5.3.2.5 Reusability and Shelf life

The cyclic performance of our IDE sensor was carried out by reusing the sensor for 3 cycles (Table-5.5). When the sensor was reused with the target analyte of 5 ppm limonin (standard), the C^S_{sam} value after the 1st cycle, 2nd cycle and 3rd cycle was degraded by 11.20 %, 47.15 % and 70.42 % respectively from its initial value. The curve (Fig. 5.10a) shows the decreasing trend of capacitance with SD of ± 1.8 when the sensor was reused for the stated cycles. A high decrease in slope was observed after the use of the sensor for 1st cycle.

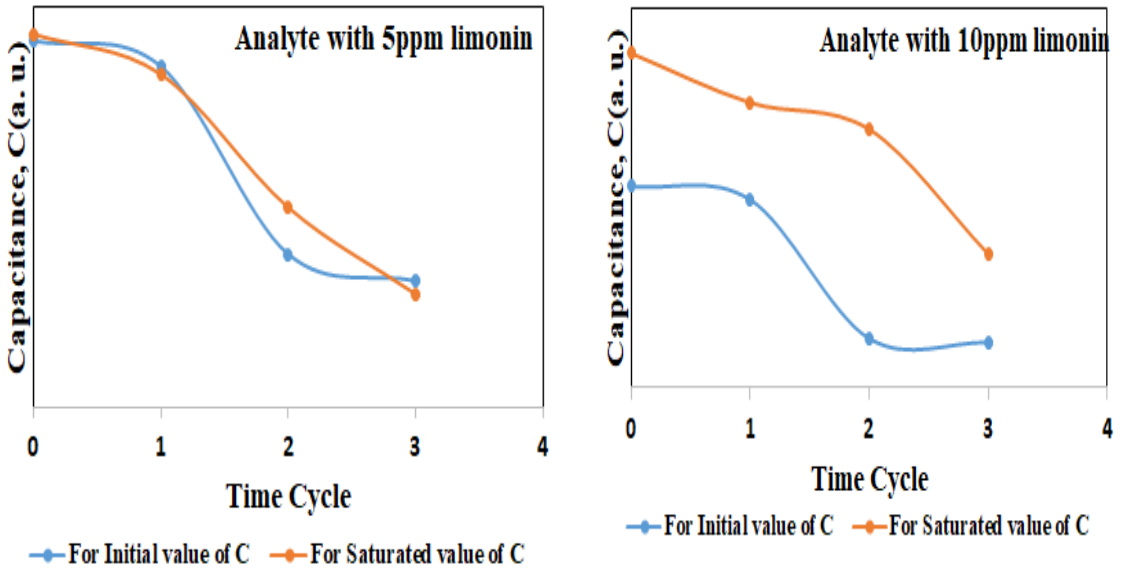

(a) (b)

Figure 5.10: Reusability of sensors (a) sensor tested with 5 ppm limonin standard (b sensor tested with 5 ppm limonin standard

Similarly, when tested with 10 ppm of limonin, the sensor performance was degraded by 13.84 %, 21 % and 60.04% after the 1st cycle, 2nd cycle and 3rd cycle respectively from its initial reading with a SD of ±2.24. The decrease in Capacitance is also depicted in Fig. 5.10b. Hence sensor can be reused for 1st cycle with degradation in the value of approximately 11.20 %. Afterward, due to the use of an inexpensive flexible paper substrate, the initial capacitance of the sensor decreases tremendously in its response leading to inaccuracy in measurement. But we can repeatedly use our sensor system by simply replacing the low-cost sensor only with the new one.

Table 5.5: Reusability of IDE sensor

Analyte	Cycle no	C_{in} (Initial value before measurement)		C^s_{sam}	
		Capacitance value (pF)	Percentage degraded (approximate)	Capacitance value(pF)	Perc. degraded (approximate)
5 ppm	First use of sensor	5.50	0%	5.59E+07	0%
	1st cycle of sample exposure	5.12	6.9 %	4.97E+07	11.20 %
	2nd cycle of sample exposure	2.3	58.18%	2.95E+07	47.15 %
	3rd cycle of sample exposure	1.9	65.45 %	1.65E+07	70.42 %
10ppm	First use of sensor	5.30	0%	8.82E+07	0%
	1st cycle of sample exposure	4.95	6.6%	7.60E+07	13.84 %
	2nd cycle of sample exposure	1.3	75%	6.90E+07	21 %
	3rd cycle of sample exposure	1.2	77 %	3.52E+07	60.04%

We have also tested the self-life of the sensor for 12 and 24 weeks (Table 5.6) exhibiting ~ 11% and 44% degradation of the initial capacitance value of the sensor respectively. More degradation after 12 weeks is due to the degradation of the Ag paint IDE structure and degradation of the sensing layer formed on the paper substrate.

Table 5.6: Shelf life of the sensor

Sensor no.	Cycle no(approx. time)	C_{in} (Initial value pF)	Percentage degraded (approximate)
sensor1	First use of sensor	5.55	0%
	After 3 months	4.956	11%
	After 6 months	2.979	46.32%
Sensor2	First use of sensor	6.13	0%
	After 3 months	4.95	19.24%
	After 6 months	3.408	44.40%
Sensor3	First use of sensor	5.23	0%
	After 3 months	4.711	9.92%
	After 6 months	3.315	36.61%

5.4 Comparison with reported methods/devices

In terms of reaction time, the limit of detection (LOD), selectivity, sensitivity, reusability, and flexibility, the current IDE-based sensor was compared with the earlier reported sensors in detecting limonin in citrus fruit juices (Table 5.7) [12, 22-24]. The odorant-binding protein-modified screen-printed electrodes do not show specificity to limonin and assess the bitterness of fruit juice as a whole with a very low LOD of 10 nM. The organic transistor shows a high detection limit as compared to our developed sensor. The surface molecularly imprinted polymers (SMIPs) exhibit only debittering of limonin, taking a time of ~5 min. The electrochemical device introduced by Puri et al. takes a much longer time (~20 min) for its response compared to the present sensor based on IDE. As reported the OECT sensor/device can be reused but needs deposition of its sensing material every time it is reused. Our flexible device can be used repeatedly by just replacing the inexpensive sensor. Onsite monitoring remains a vital issue for the sensors. The previously reported devices/ sensors need a sophisticated measuring device such as an impedance analyzer for their output measurement which is bulky as well as not suitable for onsite monitoring. This limitation is overcome by our portable Arduino-based measuring setup integrated with the sensor. The OECT, amperometric biosensor uses complex fabrication steps whereas the present work requires simple fabrication procedures. A simple fabrication process here helps in the requirement of not highly

skilled professionals. Moreover, mass production of the present sensors can be achieved at a low cost which makes it advantageous in comparison to other techniques listed in Table 5.7. Hence compared to earlier works, our developed sensor shows considerable advantages which make it suitable for monitoring limonin in citrus fruit juices

Table 5.7: Comparative study with previously reported devices

Device	selectivity	Sensitivity	Response/ detection time	Detection limit	reusability	flexibility
Organic electrochemical transistor (OECT) based on ceria nanoparticles integrated fibroins	selective	10.41 ± 0.35 μA/ μM	response time in seconds	10 nM	recycled several times by replacing the CNPs-SF and PEDOT:PSS layers	Not flexible
Amperometric biosensor using Mutant (lim+) of a strain Pseudomonas putida G7	selective	-------	20 min for the steady-state method and 12 min for the initial slope method	----	Reusable	Not flexible
Odorant-Binding Protein-Modified Screen-Printed Electrodes (device use for Detection of Bitter Taste Molecules)	Not selective	10−9 mg/mL (about 10−12 M)	---	10nM	Not reusable	Not flexible
Surface molecularly imprinted polymers (SMIPs) based debittering of limonin using SMIPs	Selective debittering		No detection but debittering time ~ 6 min			
Present work IDE based capacitive sensor using $Ce0_2$	selective	~ 9.62 ±0.095 μF/ ppm	response time ~ 13 s	5.462 μM, ~ 100ppb as obtained experimentally	Reusable up to 1st cycle after washing and drying	flexible

In this chapter, the monitoring of limonin content (causing delayed bitterness in citrus fruit juices) is achieved but the reduction of limonin is also required for the acceptability

of the fruit juice. In the next chapter, we try to discuss monitoring and reduction of limonin in citrus fruit juices.

5.5 Summary

A novel CeO_2 NPs based interdigitated electrode capacitive sensor has been designed and fabricated for measuring limonin concentration to monitor bitterness in citrus fruit juices. Two fruit juices sample namely- Citrus limetta and Citrus grandis were investigated for limonin concentration. The IDE capacitive sensor shows an excellent specificity of measurement of limonin in fruit juices with a sensitivity of ~ 9.62 ±0.095 µF/ppm, a very fast response time of ~ 13 s and reusability with less than 13.8 % degradation of initial capacitance value after one cycle. The sensor's performance was validated using HPLC analysis, a conventional method of quantification. An accuracy (in terms of percentage error) of 5.20% and 14.9% were achieved for the sensor for the quantification of limonin in Citrus limetta and Citrus grandis fruit juices respectively. The low-cost flexible paper substrate-based capacitive sensor assures easy and rapid onsite monitoring of limonin during the preservation of fruit juice with environmentally–friendly and easy disposal capability.

As discussed, we are required to have both monitoring of limonin content and measurement of its reduction to an acceptable limit in fruit juices. In chapter 6, we tried to mention both the detection and reduction measurement of limonin using the IDE device fabricated with magnesium silicate.

Bibliography

[1] Sheppard, N. F., Tucker, R. C. and Wu, C. Electrical conductivity measurements using microfabricated interdigitated electrodes. *Analytical Chemistry*, 65(9):1199-1202, 1993.

[2] Mukhopadhyay, S. C. Sensing and instrumentation for a low cost intelligent sensing system. In *2006 SICE-ICASE International Joint Conference*, pages 1075-1080, 2006. IEEE.

[3] Leng, X., Li, W., Luo, D. and Wang, F. Differential structure with graphene oxide for both humidity and temperature sensing. *IEEE Sensors Journal*, 17(14):4357-4364, 2017.

[4] Gong, H., Zhao, C. and Wang, F. On-chip growth of SnO 2/ZnO core–shell nanosheet arrays for ethanol detection. *IEEE Electron Device Letters*, 39(7):1065-1068, 2018.

[5] Wang, Y., Leng, X., Zhao, C. and Wang, F. Tunable Humidity-Sensing Performance of Graphene Oxide With Leaf-Vein-Like Multiwall Carbon Nanotube Conductive Networks. *IEEE Sensors Journal*, 21(17):18469-18476, 2021.

[6] Gong, H., Zhao, C., Niu, G., Zhang, W. and Wang, F. Construction of 1D/2D α-Fe2O3/SnO2 hybrid nanoarrays for sub-ppm acetone detection. *Research*, 2020, 2020.

[7] Abbasi, S., Zandi, P. and Mirbagheri, E. Quantitation of limonin in Iranian orange juice concentrates using high-performance liquid chromatography and spectrophotometric methods. *European Food Research and Technology*, 221(1):202-207, 2005.

[8] Kupiec, T. Quality-control analytical methods: High-performance liquid chromatography. *International journal of pharmaceutical compounding*, 8:223-227, 2004.

[9] Korsvik, C., Patil, S., Seal, S. and Self, W. T. Superoxide dismutase mimetic properties exhibited by vacancy engineered ceria nanoparticles. *Chemical communications*, (10):1056-1058, 2007.

[10] Singh, K. R., Nayak, V., Sarkar, T. and Singh, R. P. Cerium oxide nanoparticles: properties, biosynthesis and biomedical application. *RSC advances*, 10(45):27194-27214, 2020.

[11] Tsunekawa, S., Sivamohan, R., Ohsuna, T., Takahashi, H. and Tohji, K. Ultraviolet absorption spectra of CeO2 nano-particles. In *Materials Science Forum*, volume 315, pages 439-445, 1999. Trans Tech Publ.

[12] Saraf, N., Barkam, S., Peppler, M., Metke, A., Vázquez-Guardado, A., Singh, S., Emile, C., Bico, A., Rodas, C. and Seal, S. Microsensor for limonin detection: An indicator of citrus greening disease. *Sensors and Actuators B: Chemical*, 283:724-730, 2019.

[13] Breksa, A. P. and Manners, G. D. Evaluation of the antioxidant capacity of limonin, nomilin, and limonin glucoside. *Journal of agricultural and food chemistry*, 54(11):3827-3831, 2006.

[14] Flora, S. J. Structural, chemical and biological aspects of antioxidants for strategies against metal and metalloid exposure. *Oxidative medicine and cellular longevity*, 2(4):191-206, 2009.

[15] Yuan, Z., Li, R., Meng, F., Zhang, J., Zuo, K. and Han, E. Approaches to enhancing gas sensing properties: a review. *Sensors*, 19(7):1495, 2019.

[16] Zhou, T., Sang, Y., Wang, X., Wu, C., Zeng, D. and Xie, C. Pore size dependent gas-sensing selectivity based on ZnO@ ZIF nanorod arrays. *Sensors and Actuators B: Chemical*, 258:1099-1106, 2018.

[17] Afzal, A., Iqbal, N., Mujahid, A. and Schirhagl, R. Advanced vapor recognition materials for selective and fast responsive surface acoustic wave sensors: A review. *Analytica Chimica Acta*, 787:36-49, 2013.

[18] Wusiman, M. and Taghipour, F. Methods and mechanisms of gas sensor selectivity. *Critical Reviews in Solid State and Materials Sciences*, 47(3):416-435, 2022.

[19] Ladaniya, M. and Mahalle, B. C. Fruit maturation and associated changes in'Mosambi'orange (Citrus sinensis). *Indian Journal of Agricultural Sciences*, 81(6):494-499, 2011.

[20] Kumar, N. and Goyal, R. N. Nanopalladium grained polymer nanocomposite based sensor for the sensitive determination of melatonin. *Electrochimica Acta*, 211:18-26, 2016.

[21] Kumar, U. and Yadav, B. Development of humidity sensor using modified curved MWCNT based thin film with DFT calculations. *Sensors and Actuators B: Chemical*, 288:399-407, 2019.

[22] Puri, R., Malik, M. and Ghosh, M. An amperometric biosensor developed for detection of limonin levels in kinnow mandarin juices. *Annals of microbiology*, 62(3):1301-1309, 2012.

[23] Chen, Z., Zhang, Q., Shan, J., Lu, Y. and Liu, Q. Detection of Bitter Taste Molecules Based on Odorant-Binding Protein-Modified Screen-Printed Electrodes. *ACS omega*, 5(42):27536-27545, 2020.

[24] Zhang, J.-W., Tan, L., Zhang, Y.-Z., Zheng, G.-C., Xia, Z.-N., Wang, C.-Z., Zhou, L.-D., Zhang, Q.-H. and Yuan, C.-S. Debittering of lemon juice using surface molecularly imprinted polymers and the utilization of limonin. *Journal of Chromatography B*, 1104:205-211, 2019.